Available online at www.sciencedirect.com
ScienceDirect
Inorganica Chimica Acta 359 (2006) 4335–4342
Inorganica Chimica Acta
www.elsevier.com/locate/ica

In vitro antitumor activity and interaction with DNA model bases of *cis*-[$PtCl_2$(iPram)(azole)] complexes and comparison with their *trans* analogues

Elena Pantoja [a], Agata Gallipoli [a], Steven van Zutphen [a], Duncan M. Tooke [b], Anthony L. Spek [b], Carmen Navarro-Ranninger [c], Jan Reedijk [a,*]

[a] *Leiden Institute of Chemistry, Gorlaeus Laboratories, Leiden University, P.O. Box 9502, 2300 RA, Leiden, The Netherlands*
[b] *Utrecht University, Crystal and Structural Chemistry, Padualaan 8, 3584 CH, Utrecht, The Netherlands*
[c] *Departamento de Química Inorgánica, Universidad Autónoma de Madrid, Crtra de Colmenar Viejo Km. 15, 28049 Madrid, Spain*

Received 23 May 2006; accepted 4 June 2006
Available online 17 June 2006

Abstract

Asymmetric *cis*-platinum(II) complexes with isopropylamine and two different azole ligands were synthesized and characterized with different techniques. In addition, for one of the complexes the X-ray structure was determined. Cytotoxicity tests using several human tumor cell lines, including the cisplatin-sensitive cell line A2780 and its cisplatin-resistant analogue. These results were compared with the results obtained for the *trans* isomers of the presented complexes and a relation between the structure and the activity was established. It was found that complexes with *cis* geometry are less active than their *trans* analogues, in particular in the resistant cell line A2780R. However, complex **1** can overcome cisplatin resistance to a certain extent. In the interaction with GMP, the asymmetric *cis*-Pt(II) complexes react with similar rates as their *trans* analogues and they behave as bifunctional species.

Keywords: Platinum(II); Planar ligands; Amines; Cytotoxic activity; DNA model bases

1. Introduction

It is well known that cisplatin, unlike transplatin possesses antitumor activity [1]. The later is merely toxic [2]. However, recent examples show that – by carefully choosing the non-leaving group ligands for transplatin analogues – one can obtain highly cytotoxic compounds, which retain their activity in tumors resistant to cisplatin [3–7]. Along these lines we have recently published a series of asymmetric transplatin analogues compromising an azole and an isopropylamine ligand showing remarkable cytotoxic activity. We believe the activity of these complexes to be related to the kinetics of binding to the DNA, as studied by the interaction with the model base 5′-GMP. Indeed reaction kinetics comparable to cisplatin were observed for the transplatin analogues [8]. Conversely, transplatin itself reacts with 5′-GMP much slower [2]. Apparently the steric hindrance around the central platinum atom introduced by the combination of the isopropylamine and the azole ligands render the platinum complexes cytotoxic. However, the geometry of a complex will also influence greatly how it coordinates to DNA inside the tumor cells; thus it plays an important role in the cytotoxicity. To evaluate the importance of geometry in the cytotoxic activity of our transplatin complexes, we decided to prepare their *cis* analogues (Fig. 1) for cytotoxicity and further DNA binding and structural studies.

In the present paper we describe the synthesis, characterization, in vitro cytotoxicity and reactivity towards GMP of two new asymmetric platinum complexes composed of azole ligands (i.e. 1-methylimidazole (Meim) and

* Corresponding author. Tel.: +31 71 527 4459; fax: +31 71 527 4671.
E-mail address: reedijk@chem.leidenuniv.nl (J. Reedijk).

0020-1693/$ - see front matter © 2006 Elsevier B.V. All rights reserved.
doi:10.1016/j.ica.2006.06.012

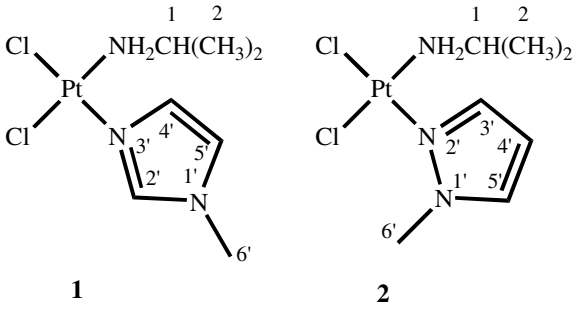

Fig. 1. Structural formula and used atom numbering of the new asymmetric *cis*-Pt(II) complexes.

1-methylpyrazole (Mepz)) and an isopropylamine (iPram) ligand in *cis* geometry.

2. Experimental

2.1. Materials and measurements

K_2PtCl_4 was provided by Johnson & Matthey (Reading, UK). Isopropylamine, sodium perchlorate, perchloric acid and guanosine 5′-monophosphate (GMP) were obtained from Sigma–Aldrich. 1-Methylimidazole and 1-methylpyrazole were obtained from Fisher Scientific Nederland B.V.

Elemental analysis was performed on a Perkin–Elmer series II CHNS/O Analyzer model 2400. NMR spectra were recorded on a Bruker DPX 300. The temperature was kept constant (at 298 K for the characterization of the complexes and at 310 K for the GMP reactions) by a variable temperature unit. ^{1}H and ^{195}Pt NMR was measured in acetone-d_6 (for the intermediate diiodo complexes), DMSO (for the characterization of the final complexes) and D_2O (for the reactions with GMP). FTIR spectra were obtained on a Perkin–Elmer Paragon 1000 FTIR spectrophotometer equipped with a Golden Gate ATR device, using the diffuse reflectance technique in the range 4000–300 cm^{-1} (resolution 4 cm^{-1}). Mass spectrometry was performed on a Finnigan TQS700 instrument.

2.2. Synthesis of the complexes

The synthesis of both complexes was accomplished in four steps as presented in Scheme 1 [9]. Details of the synthesis are given below.

2.2.1. *cis*-[PtI_2(iPram)$_2$]

K_2PtCl_4 (2.0 g, 4.82 mmol) was dissolved in 100 ml of water and treated with 8.0 g (47 mmol) of KI. The solution was stirred for 1.5 h at room temperature. Two equivalents of iPram (0.57 g, 9.64 mmol) were added to the K_2PtI_4 solution. The reaction mixture was stirred for 3 h. The yellow precipitate was washed with water, methanol and diethyl ether. The final product *cis*-[PtI_2(iPram)$_2$] was dried in air. Yield: 2.61 g (95%). ^{1}H NMR (acetone-d_6): δ (ppm): 4.37 (4H, s^{br}); 3.57 (2H, sept, 6.69 Hz), 1.37 (12H, d, 6.5 Hz).

2.2.2. [PtI_2(iPram)]$_2$

A suspension of *cis*-[PtI_2(iPram)$_2$] (2.61 g, 4.60 mmol) in 24 ml of water and 74 ml of ethanol was treated with 4.67 ml of $HClO_4$ (70%) over a period of 9 days. During the reaction the yellow precipitate turned into a red brown precipitate. The suspension was filtered and the precipitate washed with water and dried in air. Yield: 2.18 g (93%). ^{1}H NMR (acetone-d_6): δ (ppm): 4.47 (4H, s); 3.24 (2H, sept, 6.46 Hz); 1.38 (12H, d, 6.46 Hz). ^{195}Pt NMR, δ (ppm, acetone-d_6): −4201.9 and −4213.8.

2.2.3. *cis*-[PtI_2(iPram)(azole)]

A suspension of *cis*-[PtI_2(iPram)]$_2$ (2.16 g, 2.14 mmol) in 4.5 ml of water was mixed with 2 equiv. of azole [4.28 mmol of Meim (**i1**) and Mepz (**i2**), respectively]. The reaction mixture was stirred for 2 days at room temperature. The yellow precipitate was filtered, washed with water, and dried in air. Yield: (**i1**) 0.84 g (73%); (**i2**) 1.0 g (85%). ^{1}H NMR (acetone-d_6): δ (ppm): (**i1**) 3.0 [s, 1H, $NH_2CH(CH_3)_2$], 1.27 [d, 6H, $NH_2CH(CH_3)_2$], 4.64 [s^{br}, 2H, $NH_2CH(CH_3)_2$], 8.18 [s, 1H, $_{Meim}NCHN$], 7.28 [d, 1H, $_{Meim}NCHCH$], 7.8 [d, 1H, $_{Meim}CHCHN$], 3.88 [s, 3H, $_{Meim}NCH_3$]; ^{195}Pt NMR (acetone-d_6): δ (ppm):

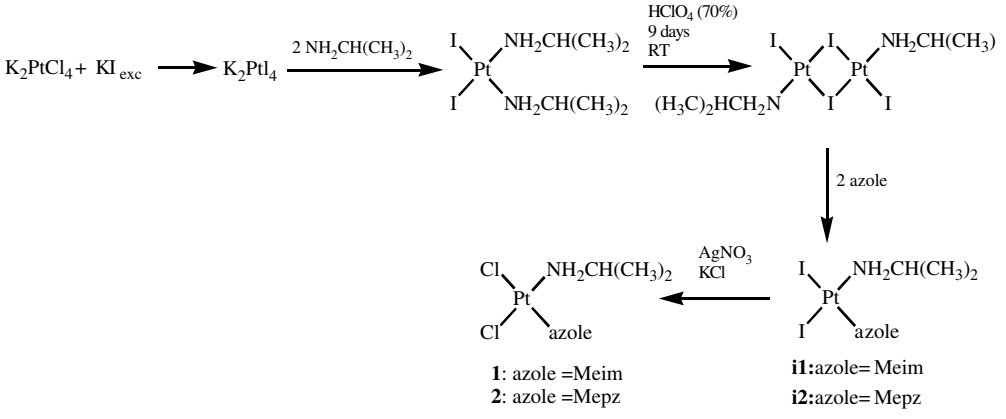

Scheme 1. Reaction scheme of complexes *cis*-[$PtCl_2$(iPram)(azole)] (azole = Meim (**1**) and Mepz (**2**)) (exc = excess, RT = room temperature).

−3238. ^{1}H NMR (acetone-d_6): δ (ppm): (**i2**) 3.1 [s, 1H, $NH_2CH(CH_3)_2$], 1.35 [d, 6H, $NH_2CH(CH_3)_2$], 4.85 [s^{br}, 2H, $NH_2CH(CH_3)_2$], 7.82 [d, 1H, $_{Mepz}NCHCH$], 6.48 [t, 1H, $_{Mepz}CHCHCH$], 7.98 [d, 1H, $_{Mepz}CHCHN$]; ^{195}Pt NMR (acetone-d_6): δ (ppm): −3332.

2.2.4. *cis*-[$PtCl_2$(iPram)(azole)]

A suspension of *cis*-[PtI_2(iPram)(azole)] in 80 ml of water was treated with 1.85 equiv. of $AgNO_3$ for 1 day in the dark. Precipitated AgI was filtered off and 4 equiv. of KCl was added to the filtrate. The reaction mixture was stirred for 10 h at 40 °C and allowed to stay 1 day at 4 °C. When the mixture was cooled a yellow solid precipitated. The solid was filtered, washed with water, and dried in air. A second fraction was obtained by evaporating half of the solvent, and filtering off the precipitate. Yield: (**1**) 0.1907 g (34%), (**2**) 0.248 g (36%).

The resulting complexes, *cis*-[$PtCl_2$(iPram)(Meim)] (**1**) and *cis*-[$PtCl_2$(iPram)(Mepz)] (**2**) (Fig. 1), were characterized by ^{1}H and ^{195}Pt NMR (Table 1), and by elemental analysis. Data for elemental analysis are: (**1**) Theory % ($PtCl_2C_7H_{15}N_3$): C, 20.65; H, 3.71; N, 10.32. Found: C, 20.54; H, 3.80; N, 10.43%. (**2**) Theory % ($PtCl_2C_7H_{15}N_3$): C, 20.65; H, 3.71; N, 10.32. Found: C, 20.74; H, 3.90; N, 10.53%.

2.3. X-ray structural determination for complex *1*

Single crystals of complex **1** were obtained directly from the mother solution in water at 4 °C. Reflections were measured on a Nonius Kappa CCD diffractometer at a temperature of 150(2) K. The structure was solved with automated Patterson methods (DIRDIF-99) [10] and refined with SHELXL-97 [11] against F^2 of all reflections. Hydrogen atoms were introduced at calculated positions, after being confirmed in a difference map, and refined riding on their carrier atom. Molecular illustration, structure checking and all calculations were performed with the PLATON package [12,13]. The details of the crystal structure determination are presented in Table 2, and the CIF file has been deposited with Cambridge Structural Database with reference No. CSD 279490.

Table 1
^{1}H and ^{195}Pt NMR data for the *cis*-[$PtCl_2$(iPram)(azole)] complexes (solvent: DMSO-d_6) (see Fig. 1 for numbering)

	iPram	**1**	**2**
H1	2.95 sept 1H	2.57 (1H, sept)	Under H_2O (from DMSO)
H2	0.92 d 6H	1.11 (6H, d)	1.27 (6H, d)
NH_2	2.10 2H s^{br}	4.74 (2H, s^{br})	4.85 (2H, s^{br})
H1′		3.71 (3H, s)	4.34 (3H, s)
H2′		8.10 (1H, s)	
H3′			7.89 (1H, s)
H4′		7.26 (1H, d)	6.45 (1H, d)
H5′		7.16 (1H, d)	8.10 (1H, s)
δ (^{195}Pt), ppm		−2090	−2126

s^{br}: broad singlet, d: doublet, t: triplet, sept: septuplet.

Table 2
Crystal data for complex *cis*-[$PtCl_2$(iPram)(Meim)] (**1**)

	1
Chemical formula	$[PtCl_2C_7H_{15}N_3]$
Formula weight	407.21
Crystal system	orthorhombic
Space group	$P2_12_12_1$
a (Å)	8.0479(4)
b (Å)	10.3954(3)
c (Å)	14.0445(10)
$\alpha = \beta = \gamma$ (°)	90
V (Å^3)	1174.98(11)
Z	4
ρ_{calc} (g/cm^3)	2.3019(2)
μ (mm^{-1})	12.359
Transmission	0.13–0.29
Crystal color	colorless
Crystal size (mm^{-3})	$0.10 \times 0.15 \times 0.20$
Number of reflections measured	21 622
Number of unique reflections	2680
Number of observed reflections [$I > 2\sigma(I)$]	2580
Number of parameters	121
R_1 (all reflections)	0.0182
R_1 (observed reflections)	0.0163
wR_2 (all reflections)	0.0344
S	1.07
Flack parameters	0.013(7)
Minimum/maximum residual density (e A^{-3})	−0.88/1.23

2.4. Cytotoxicity tests: cell lines and culture conditions

Cell lines WIDR, M19, A498, IGROV and H226 belong to the currently used anticancer screening panel of the National Cancer Institute, USA [14]. The MCF7 cell line is estrogen (ER)+/progesterone (pgR)+ and the cell line EVSA-T is (ER)−/(pgR)−.

All cell lines were maintained in a continuous logarithmic culture in RPMI 1640 medium with Hepes and phenol red. The medium was supplemented with 10% FCS, penicillin 100 IU/ml and streptomycin 100 μg/ml. The cells were mildly trypsinized for passage and for use in the experiments. The cytotoxicity in these human cell lines was estimated by the microculture sulforhodamine B (SRB) test [15]. Each of the complexes (1 mg), **1** and **2**, were initially dissolved in DMSO. A threefold aqueous dilution sequence of ten steps was used in quadruplicate. Cell survival was evaluated by measuring the absorbance at 540 nm using an automated microplate reader (Labsystems Multiskan MS).

The cell lines A2780 and A2780R, i.e. ovarian cancer cell lines derived from untreated patients [16], were maintained in continuous logarithmic culture Dulbecco's modified Eagle's Medium (DMEM) (Gibco BRL™, Invitrogen Corporation, NL) supplemented with 10% fetal medium serum (Perbio Science, Belgium), PenicillinG Sodium (100 U/ml Duchefa Biochemie BV, NL), Streptomycin (100 μg/ml Duchefa Biochemie BV, NL) and Glutammax 100× (Gibco BRL™, NL). Cells, which survive in cultures treated with the compounds, were evaluated using the so-called MTT

method [17]. Compounds were added in microwells containing the cell culture at final concentrations of 0–200 μM; 48 h later, cell survival was evaluated by measuring the absorbance at 520 nm, using a BIO-RAD microplate model 550. The IC_{50} values (i.e. the concentration of the complex that restricts cell growth to 50% of that compared with the control) were calculated from curves constructed by plotting cell survival (%) versus compound concentration (μM). All experiments were carried out in triplicate.

2.5. Reactions of complexes 1 and 2 with GMP

The complexes **1** and **2** were reacted with an excess (1:4) of GMP in 250 μl of 0.1 M $NaClO_4/D_2O$ at 310 K in an NMR tube. Both complexes were first pre-dissolved in 30 μl of DMF-d_7, because of the poor solubility of the complexes in water, followed by the addition of 480 μl of 0.1 M $NaClO_4/D_2O$. The reactions were left to incubate at 310 K in the dark. The reactions were studied by ^1H NMR, recording spectra at time intervals of 30 min during the overnight reaction, and after every 24 h, until no further changes were observed. Subsequently, at the end of the reactions, ^{195}Pt NMR spectra were recorded from the same solution in the same NMR tube and a mass spectrometry analysis was performed.

3. Results and discussion

3.1. Synthesis and characterization

Preparation of the *cis*-Pt(II) compounds involves obtaining the iodine-bridged dimer with isopropylamine and the subsequent breaking of the bridge with the different azole ligands [9,18]. Elemental analysis, infrared spectra and ^1H, ^{13}C and ^{195}Pt NMR spectra and mass spectrometry confirm the formation of the intermediate diiodo and the final compounds. Data for elemental analysis are in agreement with the empirical formulas $PtCl_2C_7H_{15}N_3$ for both complexes **1** and **2**. IR spectra support the *cis* geometry of both complexes, as seen from the appearance of two different bands assigned to the Pt—Cl stretching bond [19] at 330 and 324 cm^{-1}, 333 and 321 cm^{-1}, for **1** and **2**, respectively. The IR spectra also show bands at 435, 414 cm^{-1}, respectively, which can be assigned to the asymmetric Pt—N stretch [19]. In this case splitting due to a *cis* orientation remains unresolved. The ^1H and ^{195}Pt NMR (Table 1) data agree with the structures of the complexes proposed by IR data. For a final confirmation a 3D-structure determination has been carried out for compound **1**, which is described below.

3.2. X-ray structure of complex cis-[PtCl2(iPram)(Meim)] (1)

Compound **1** crystallizes in the orthorhombic space group $P2_12_12_1$ with $Z = 4$. A molecular plot of the structure is presented in Fig. 2. Selected bond lengths and angles are given in Table 3. The coordination of the Pt atom is square planar (angles sum 360.04). The Pt—N distances are in the expected range, with the Pt—N(amine) distances only slightly longer (2.048(3) Å) than the Pt—N(azole) distances (2.003(3) Å). The torsion angles in this complex, amount to 54.6(3) and −71.3(3) for Cl2PtN3C2 and Cl2Pt1N7C8, respectively, and are quite different from that of its *trans* analogue [8]. In the case of the *cis*-Pt(II) the angles show a perpendicular disposition respect to the equatorial plane formed by Cl1, Cl2, N3 and N7, while in the case of the *trans* analogues both ligands, isopropylamine and 1-methylimidazole, are almost in the equatorial plane, only in the case of one of the residues the iPram ligand shows similar torsion angle as the *cis* complex [8].

The lattice structure consists a zig-zag one-dimensional chain formed in the direction of the crystallographic *a* axis. A plot of the hydrogen-bonding pattern in the chain is displayed in Fig. 3. The details for the hydrogen bonding geometry are given in Table 4. As it can be observed, one of the hydrogen bonds, i.e. N7—H7A...Cl2 is quite weak with a Cl...N distance of 3.666(3) Å, whereas the other is quite strong (Cl...N = 3.30 Å).

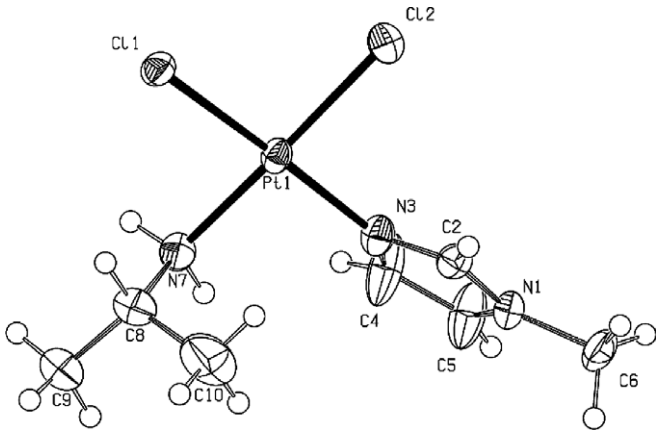

Fig. 2. Molecular structure and of the complex *cis*-[$PtCl_2$(iPram)(Meim)] (**1**).

Table 3
Selected bond distances (Å), angles, and relevant torsion angles (°) for *cis*-[$PtCl_2$(iPram)(Meim)] (**1**)

Atoms	Distances and angles
Pt1—N7	2.048(3)
Pt1—N3	2.003(3)
Pt1—Cl1	2.296(9)
Pt1—Cl2	2.315(11)
N3—Pt1—N7	91.43(13)
Cl1—Pt1—Cl2	92.07(3)
N3—Pt1—Cl2	89.59(9)
N7—Pt1—Cl1	86.95(9)
N7—Pt1—Cl2	178.00(9)
N3—Pt1—Cl1	177.92(9)
Cl2—Pt1—N3—C2	54.6(3)
Cl1—Pt1—N7—C8	−71.3(3)

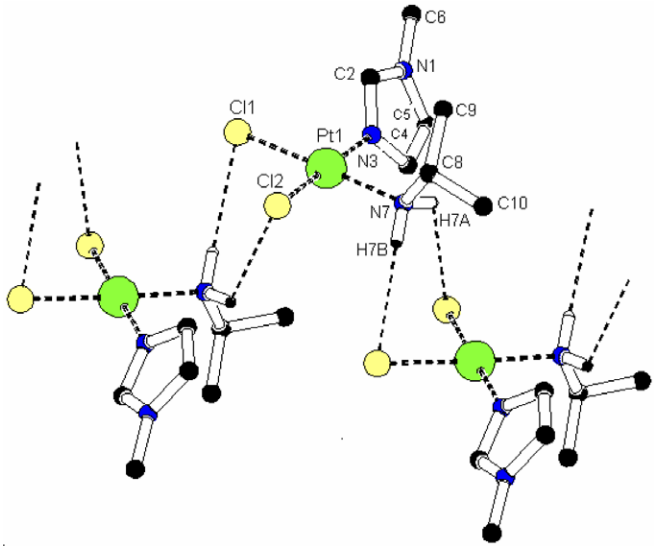

Fig. 3. Intramolecular hydrogen bonding between N—H and Cl in *cis*-[$PtCl_2$(iPram)(Meim)]. C—H hydrogen atoms have been omitted for clarity.

Table 4
Hydrogen bonding parameters for *cis*-[$PtCl_2$(iPram)(Meim)] (**1**)

D–H...A	D–H (Å)	H...A (Å)	D...A (Å)	D–H...A (°)
N7—H7A...Cl2^{i}	0.92	2.75	3.666(3)	175
N7—H7B...Cl1^{i}	0.92	2.80	3.300(3)	116

Symmetry operation: $^{i}-1/2+x, 3/2-y, -z$.

3.3. Reactions of complexes *1* and *2* with GMP

The reaction of complexes **1** and **2** with an excess of GMP (1:4) is illustrated in Scheme 2. During the reactions ^{1}H NMR spectra were taken every 30 min for 24 h then every 12 h. Careful monitoring of the H8 proton shift of the GMP allowed us to observe the appearance and disappearance the different platinum-GMP species formed in the reaction as illustrated in Fig. 4.

Both complexes behave as bifunctional species, giving rise to the complete formation of the bisadduct product (**I**$(GMP)_2$ and **II**$(GMP)_2$, Scheme 2) within 48 h. At the end of the reaction (48 h) two different signals at 8.34 and 8.50 ppm and 8.33 and 8.59 ppm are observed for complexes **1** and **2**, respectively. This is because of the asymmetric nature of the complexes as reported earlier [9]. ^{195}Pt NMR confirms the formation of these bisadduct species, showing a signal at −2379 and −2375 ppm for complexes **1** and **2**, respectively. These chemical shifts are 100 ppm lower than the values commonly observed for the 4N environment around the platinum center in aqueous solution. A solvent dependence of ^{195}Pt shifts is held responsible for this difference, and such effects have also been reported in related studies [20,21]. Mass spectrometry also confirms the formation of the bisadduct products showing peaks at m/z of 531.6 and 531.7 for complex **1** and **2**, respectively. These values correspond to the mass of the bisadduct species with neutral GMP ligands.

Both H1′ signals of the sugar ring of each GMP are shifted to higher field, confirming a stacking interaction [22]. Since in both complexes, the two GMP ligands bound to the platinum are not equivalent, two different doublets would be expected in the proton NMR of each H1′ of each GMP, and in fact, this is observed. The conformation of sugar moiety of each GMP, in the bisadduct product, are mainly in the N-type population, as observed for the small coupling constants values $J_{1'-2'}$ 5.15 and 5.89 Hz for **1** and **2**, respectively [22–24]. This is the same conformation as the one observed in DNA when cisplatin forms the 1,2-intrastrand cross-links.

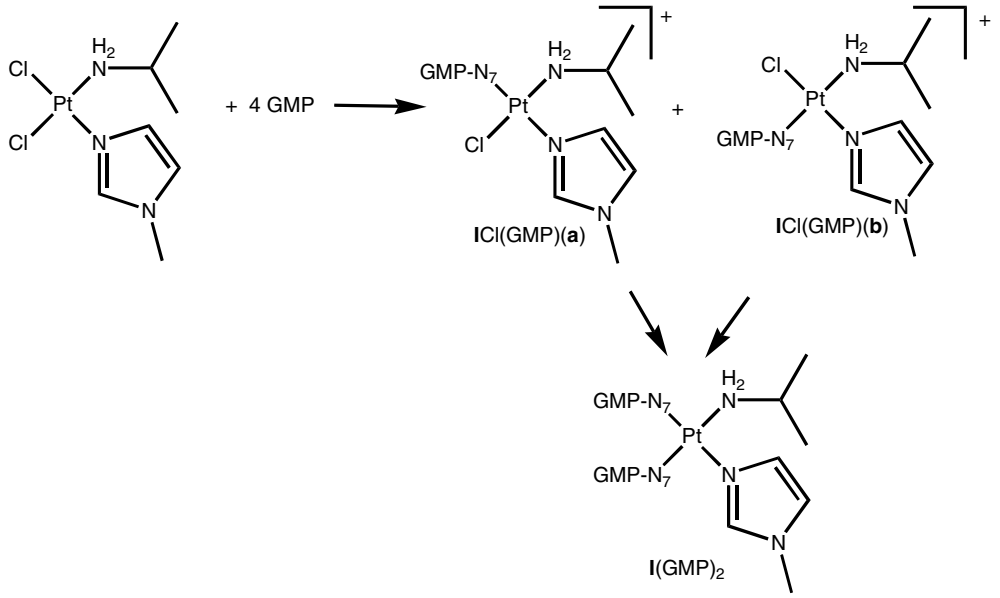

Scheme 2. Scheme of the reaction of compound **1** with GMP.

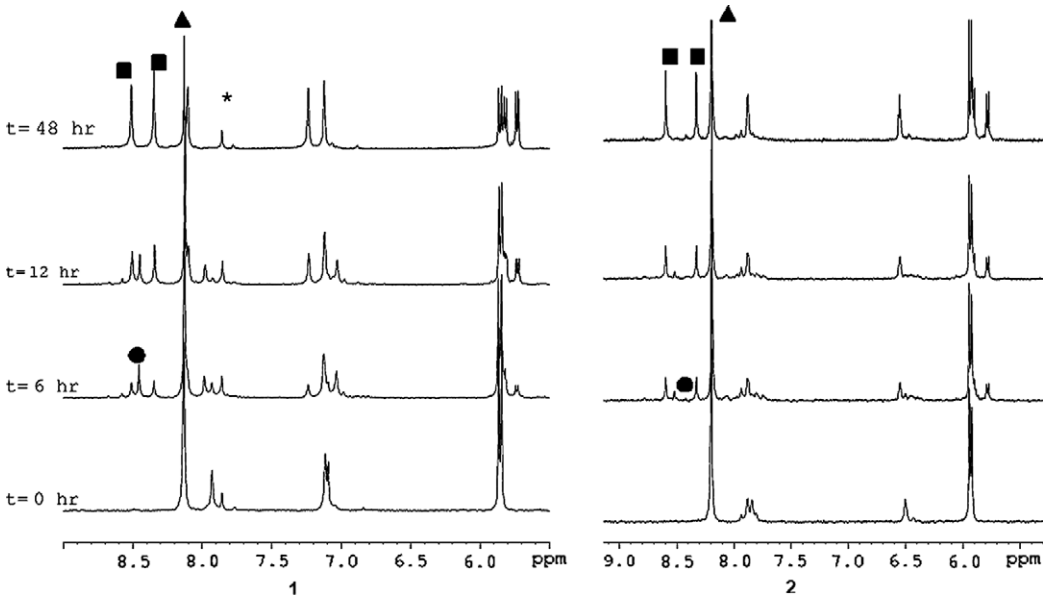

Fig. 4. ^{1}H NMR spectra in the aromatic region on the reaction of the complexes **1** and **2** with 4 equiv. of GMP in 0.1 M $NaClO_4/D_2O$ solution measured at 310 K as a function of time. The symbols show the H8 signals of GMP ligands in the products: **I**, **II** Cl(GMP) (●), **I**, **II**$(GMP)_2$ (■), free GMP (▲). (*) corresponds to traces of DMF-d_7 used to pre-dissolve the complex.

The only difference between complexes **1** and **2** in their interaction with GMP is in the formation of the monoadduct product **I**Cl(GMP) and **II**Cl(GMP). In complex **1**, the formation of this species was observed after 1 h of reaction at 8.45 ppm. This signal increased with time of reaction, reaching 25% of the total GMP. Although theoretically two different monoadducts could be formed, due to the asymmetry of the complexes, only one signal is observed. It is thought that the isomer formed is the one where the GMP is *trans* to the 1-methylimidazole ligand (**I**Cl(GMP)(**a**), Scheme 2), since changes in the resonance of the imidazole protons are observed during the first hours of the reaction. Furthermore, this is also the sterically less demanding site. In the case of complex **2**, a signal at 8.52 ppm appeared, tentatively assigned to the monoadduct product (**I**Cl(GMP)). However, this signal did not increase much, reaching only 3% of the total GMP and subsequently disappeared with time of reaction. Therefore, in complex **2**, the reaction rate from monoadduct to bisadduct is too high to allow the observation of the formation of a monofunctional species. This may be of relevant importance to the interaction of complex **2** with DNA, since the first hydrolysis is generally the determinant step of speed of the reaction [25].

*3.4. Kinetic aspects of complex **1** in its interaction with excess of GMP*

For complex **1**, it was possible to study the kinetics of its interaction with an excess of GMP. The study was performed by measuring the integrals of the ^{1}H NMR signal at 8.34 ppm assigned to one of the GMPs of the bisadduct species during the reaction of **1** with an excess of GMP in $NaClO_4$ (0.1 M)/D_2O solutions. The other signal assigned to the same product overlapped with the monoadduct species in a number of time intervals, so that its integral could not be determined accurately. After 11 h of reaction it was found that the monoadduct and the bisadduct species coexist in about the same proportion. The time of disappearance of 25% ($t_{1/4}$) of free GMP was found to be 6 h (360 min) and the time of formation of 25% ($t_{1/4}$) of **I**-$(GMP)_2$ was found to be 7 h (420 min). The reaction rate is proportional to the amount of available free GMP in the reaction mixture, which indicates that the reaction takes place by direct substitution of the Cl^- ligand by GMP, just as is found for its *trans* analogue [8].

Both isomers, *cis*- (**1**) and *trans*-[$PtCl_2$(iPram)(Meim)] [8], react completely with GMP within 48 h, they only differ in the formation time of the different intermediate species.

Table 5
In vitro cytotoxicity assay of the asymmetric *cis*-platinum(II) complexes and cisplatin on human tumor cell lines (abbreviations: see text)

Compounds	IC_{50} (μM)						
	MCF7	EVSA-T	WIDR	IGROV	M19	A498	H226
1	71.1	37.4	74	33.2	77.5	>100	>100
2	57.5	6.5	60.2	15.6	58.7	84.2	67
Cisplatin	1.42	1.42	1.78	0.43	1.84	5.75	4.53

They even react through the same mechanism, in contrast with cisplatin where the rate-determining step for binding to DNA is known to be the hydrolysis of a Pt—Cl bond [25].

3.5. Cytotoxicity properties of complexes *1* and *2*

In Table 5 the cytotoxicity data in a series of human cell lines (MCF7 and EVSA-T (breast cancer), WIDR (colon cancer), IGROV (ovarian cancer), M19 (melanoma), A498 (renal cancer), and H226 (non-small cell lung cancer)) of the complexes **1** and **2** are listed and compared to cisplatin. The IC_{50} value represents the minimum amount of drug needed to inhibit 50% of the cancer cells growth. Both *cis*-platinum(II) complexes show an antitumor activity significantly lower than that of cisplatin and even lower than their *trans* analogues [8]. The cytotoxicity of both *cis* complexes, in three of these human tumor cell lines, WIRD, A498 and H226; is lower when compared to other cell lines. Complex **2** shows better antitumor activity than complex **1**; however, the differences are quite small.

The cytotoxicity of both complexes in cisplatin-sensitive (A2780) and cisplatin-resistant (A2780R) ovarian cancer cell lines was also studied and the data are shown in Table 6. In the parental cell line, A2780, both complexes show a much lower cytotoxicity than cisplatin, 5 and 7 times less cytotoxic for complexes **1** and **2**, respectively. Complex **2**, containing 1-methylpyrazole, shows an IC_{50} value slightly higher than **1**, containing 1-methylimidazole. For the *trans*-Pt(II) analogues a similar behavior has been observed [8]. So, the fact of having a pyrazole or an imidazole ring has a small, but significant influence on the cytotoxicity of this class of complexes. It is observed that the presence of a substituent at the N of the pyrazole ring has an influence on the cytotoxic activity of the complexes. When a substituent is present at the non-coordinated N of the pyrazole ring, the antitumor activity of the complex is slightly higher [8].

In the cisplatin-resistance cell line, A2780R, both complexes **1** and **2** are less cytotoxic than cisplatin, although the difference for complex **1** compared to cisplatin is small. The resistance factor (RF) is defined as the relative ratio of IC_{50} values in both cell lines (A2780R/A2780) for both *cis* complexes in fact is lower than for cisplatin. This would suggest that both *cis* complexes could overcome cisplatin resistance. However, a complex is considered as non-cross resistance when it shows a $RF < 2$; this value is taken as a standard [26]. Therefore, only complex **1**, which has an RF value of 1.86 is considered to overcome cisplatin resistance. In comparison with its *trans* analogues, its RF value is still 2.8 times higher. In addition, the *trans* isomer showed an IC_{50} value in the cisplatin-resistant cell line lower than the *cis* complex and than cisplatin. So, indeed a *cis* analogue of cisplatin has been found to show a good antitumor activity, and more importantly it overcomes cisplatin resistance.

Table 6
In vitro cytotoxicity assay of the *cis*-platinum(II) complexes and cisplatin on A2780 ovarian cancer cell lines sensitive (A2780) and resistant (A2780R) to cisplatin

Test compound	IC_{50} (μM)		
	A2780	A2780R	RF
1	15	28	1.86
2	21	49	2.33
Cisplatin	3	24	8

4. Conclusions

In this study, the synthesis, GMP interaction and cytotoxicity properties of two new *cis*-Pt(II) complexes are reported and compared to their *trans* analogues. The crystal structure of complex **1** has been presented in detail. The crystallographic data are in agreement with the square-planar geometry of the platinum complex. The cytotoxicity of these asymmetric *cis*-platinum(II) complexes in several human cell lines was found to be lower than the cytotoxicity of cisplatin and their *trans* analogues [8]. Only complex **2** was found to show comparable cytotoxicity to that of cisplatin in the EVSA-T cell line. The cytotoxicity of both complexes in the cisplatin-sensitive (A2780) and cisplatin-resistant (A2780R) cell lines was also lower than for cisplatin and for their *trans* isomers. However, complex **1** shows non-cross resistance to cisplatin, as deduced from its RF value lower than 2. When the azole ligand is changed from Mepz to Meim, the cytotoxic activity decreases. This behavior was also found for the *trans* complexes [8]. The cytotoxicity increases when the azole is an unsubstituted pyrazole. This behavior is probably related to the position of hydrogen-bond formation.

cis- and *trans*-[$PtCl_2$(iPram)(azole)] interact with GMP at similar rates. Both *cis* complexes behave as bifunctional species. In complex **2**, the monoadduct species could not be observed as an intermediate, which implies that it immediately reacts with a second GMP to yield the bisadduct product. In case of complex **1** a monoadduct was observed with one isomer predominantly present. When the bisadduct product is formed, two different signals are observed in the NMR spectrum, for both complexes, as a consequence of the non-equivalence of the GMPs, originating from the asymmetry of the complexes.

The presented asymmetric *cis*-Pt(II) complexes show less antitumor activity than their *trans* analogues and behave as bifunctional species, as would have been expected. Complex **1**, however, overcomes cisplatin resistance. This fact can be compared to the clinically used drug oxaliplatin, which shows a lower antitumor activity than cisplatin, but overcomes cisplatin resistance [27,28]. This is an important finding in the search of new antitumor drugs, based on platinum.

Acknowledgments

The authors thank Johnson & Matthey (Reading, UK) for their generous loan of K_2PtCl_4. Also the support and

sponsorship concerted by COST Actions D20/0001/00, D20/0002/00, D20/003/01 and Spanish CYCIT (SAF 03/01700) are kindly acknowledged. This work was supported in part (M.L., A.L.S.) by the council for Chemical Sciences of the Netherlands Organization for Scientific Research (CW-NWO). The tests of the compounds were generously supported by PCN Nederland (Pharmachemie, Haarlem).

References

[1] S. Komeda, S. Bombard, S. Perrier, J. Reedijk, J.F. Kozelka, J. Inorg. Biochem. 96 (2003) 357.
[2] M.J. Cleare, J.D. Hoeschele, Bioinorg. Chem. 2 (1973) 187.
[3] N. Farrell, L.R. Kelland, J.D. Roberts, M. Van Beusichem, Cancer Res. 52 (1992) 5065.
[4] E. Khazanov, Y. Barenholz, D. Gibson, Y. Najajreh, J. Med. Chem. 45 (2002) 5196.
[5] Y. Najajreh, J. Kasparkova, V. Marini, D. Gibson, V. Brabec, J. Biol. Inorg. Chem. 10 (2005) 722.
[6] F.P. Intini, A. Boccarelli, V.C. Francia, C. Pacifico, M.F. Sivo, G. Natile, D. Giordano, P. De Rinaldis, M. Coluccia, J. Biol. Inorg. Chem. 9 (2004) 768.
[7] M. Leng, D. Locker, M.J. Giraud-Panis, A. Schwartz, F.P. Intini, G. Natile, C. Pisano, A. Boccarelli, D. Giordano, M. Coluccia, Mol. Pharmacol. 58 (2000) 1525.
[8] E. Pantoja, A. Gallipoli, S. van Zutphen, S. Komeda, D. Reddy, M. Lutz, D.M. Tooke, A.L. Spek, C. Navarro-Ranninger, J. Reedijk, J. Inorg. Biochem. (submitted for publication).
[9] E. Pantoja, A. Álvarez-Valdés, J.M. Pérez, C. Navarro-Ranninger, J. Reedijk, Inorg. Chim. Acta 339 (2002) 525.
[10] P.T. Beurskens, G. Admiraal, G. Beurskens, W.P. Bosman, S. Garcia-Granda, R.O. Gould, J.M.M. Smits, C. Smykalla, The DIRDIF Program System, Technical Report of the Crystallography Laboratory, University of Nijmegen, Nijmegen, The Netherlands, 1992.
[11] G.M. Sheldrick, SHELDXS-86. Program for Crystal Structure Solution, University of Göttingen, Göttingen, Germany, 1997.
[12] A.L. Spek, Acta Crystallogr. Sect. A A46 (1990) C34.
[13] A.L. Spek, J. Appl. Crystallogr. 36 (2003) 7.
[14] M.R. Boyd, Princ. Pract. Oncol. 3 (1989) 1.
[15] Y.P. Keepers, P.E. Pizao, G.J. Peters, J. Van Arkotte, B. Winograd, H.M. Pinedo, Eur. J. Cancer 27 (1991) 897.
[16] A. Eva, K.C. Robbins, P.R. Andersen, A. Srinivasan, S.R. Tronick, E.P. Reddy, N.W. Ellmore, A.T. Galen, J.A. Lautenberger, T.S. Papas, E.H. Westin, F. Wongstaal, R.C. Gallo, S.A. Aaronson, Nature 295 (1982) 116.
[17] M.C. Alley, D.A. Scudiero, A. Monks, M.L. Hursey, M.J. Czerwinski, D.L. Fine, B.J. Abbott, J.G. Mayo, R.H. Shoemaker, M.R. Boyd, Cancer Res. 48 (1988) 589.
[18] F.D. Rochon, Inorg. Chim. Acta 358 (2005) 3919.
[19] K. Nakamoto, P.J. McCarthy, J. Fujita, R.A. Condrate, G.T. Behnke, Inorg. Chem. 4 (1965) 36.
[20] I.M. Ismail, P.J. Sadler, ACS Symp. Ser. 209 (1983) 171.
[21] U. Bierbach, N. Farrell, Inorg. Chem. 36 (1997) 3657.
[22] C. Altona, M. Sundaral, J. Am. Chem. Soc. 95 (1973) 2333.
[23] J.H.J. Den Hartog, C. Altona, J.C. Chottard, J.P. Girault, J.Y. Lallemand, F. Deleeuw, A.T.M. Marcelis, J. Reedijk, Nucleic Acids Res. 10 (1982) 4715.
[24] K. Okamoto, V. Behnam, M.T.P. Viet, M. Polissiou, J.Y. Gauthier, S. Hanessian, T. Theophanides, Inorg. Chim. Acta-Bioinorg. Chem. 123 (1986) L3.
[25] D.P. Bancroft, C.A. Lepre, S.J. Lippard, J. Am. Chem. Soc. 112 (1990) 6860.
[26] L.R. Kelland, C.F.J. Barnard, K.J. Mellish, M. Jones, P.M. Goddard, M. Valenti, A. Beryant, B.A. Murrer, K.R. Harrap, Cancer Res. 54 (1994) 5618.
[27] A.H. Calvert, S.J. Harland, D.R. Newell, Z.H. Siddik, A.C. Jones, T.J. McElwain, S. Raju, E. Wiltshaw, I.E. Smith, J.M. Baker, M.J. Peckham, K.R. Harrap, Cancer Chemoth. Pharmacol. 9 (1982) 140.
[28] A.H. Calvert, D.R. Newell, L.A. Gumbrell, S. Oreilly, M. Burnell, F.E. Boxall, Z.H. Siddik, I.R. Judson, M.E. Gore, E. Wiltshaw, J. Clin. Oncol. 7 (1989) 1748.